

Evaluating Measurement Uncertainty in Absolute Gravimetry: an Application of the Monte Carlo Method

Walter Bich, Giancarlo D'Agostino, Alessandro Germak and Francesca Pennecci

Istituto nazionale di ricerca metrologica, INRIM

Strada delle Cacce 73, 10135 Torino (TO), Italy

Phone: +39-011-3919-919, Fax: +39-011-3919-926, Email: g.dagostino@inrim.it

Abstract – Absolute gravity measurements are based on the reconstruction of the free-falling motion of a test body in vacuum. In this paper, two large disturbing effects are studied, namely, the non-gravitational accelerations originated by rotation and translation of the flying body. Their contribution to the uncertainty of the free-fall acceleration is evaluated using the method proposed in Supplement 1 to the GUM. The analysis is specifically applied to the IMGC-02 absolute gravimeter, but can be easily extended to other instruments.

Keywords – absolute gravimetry, uncertainty, Monte Carlo method.

I. INTRODUCTION

In a modern absolute ballistic gravimeter, the dominating contribution to data scattering is due to floor vibrations. This contribution, depending on the gravimeter and on the measurement site, amounts typically to some tens of microgal ($1 \mu\text{Gal} = 1 \times 10^{-8} \text{ms}^{-2}$). For this reason, the estimate of the measurand (the free-fall acceleration) is obtained by averaging some hundreds of individual measurement results. The present accuracy limit, due to reproducibility of the results, is believed to lie at the microgal level, corresponding to about 1 part in 10^9 of the Earth's gravitational acceleration. An absolute measurement of a physical quantity requires a detailed understanding of the influence factors affecting its realization. Special attention should be given to those effects that remain almost constant during the experimental activity and therefore are difficult, or impossible, to identify and correct. A correct uncertainty evaluation should therefore include all the effects, also those that do not contribute to data scattering. In ballistic gravimetry, the two dominating effects beside floor vibrations are the centripetal acceleration and the Coriolis acceleration [1].

This paper discusses these effects in a practical case, concerning the ballistic gravimeter IMGC-02 developed and tested at the Istituto nazionale di ricerca metrologica (INRIM) [2]. The corresponding uncertainty contributions are evaluated and propagated by using a Monte Carlo method (MCM), according to the GUM, Supplement 1 [3]. With this method, a probability density function (pdf) is assigned to each of the relevant input quantities to the model, and propagated through the model itself to yield a corresponding pdf for the measurand.

The instrument and its measurement principle are described in Section II. The centripetal and Coriolis

accelerations, as well as the assignment of their pdfs, are discussed in Section III-A and III-B, respectively. The contribution of these effects to the estimate uncertainty is given in Section IV.

II. THE MEASUREMENT PRINCIPLE

Absolute ballistic gravimeters are based on the reconstruction of the vertical trajectory followed by a test body in vacuum. In particular, the IMGC-02 adopts the symmetrical rise-and-fall method, where the test body is thrown vertically upwards.

Laser interferometry is used to determine the trajectory. The flying body acts as the moving reflector M in a vertically oriented arm of a Michelson interferometer, whereas the reference reflector R is fixed to an inertial system [4] (fig. 1). The optical fringes arising from the interferometer are converted to a sinusoidal electrical signal by a photodetector. Time values corresponding to equally spaced positions of the test body during its flight are taken by timing a recurring phase of the sinusoidal signal [5].

From the law of motion of the test body, a measurement model is obtained, relating the space-time coordinates (the indications) to a number of parameters. Among the model parameters there is the measurand, i.e., the acceleration g experienced by the moving reflector during its free falling under the influence of gravity. Since the model is non-linear in the parameters, estimates are obtained by means of a recursive least-squares algorithm [6]. Formally, the measurement model should take into account also the centripetal and Coriolis acceleration. In practice, they can be evaluated separately from the adjustment, since, as it will be shown, they contribute only to the estimate uncertainty, the corrections they involve being equal to zero.

III. THE EFFECTS

Ideally, the motion of the moving reflector should be a perfect vertical translation. In practice, this is impossible to obtain due to vertical misalignment and bending moments of the launch pad. As a result, the real motion is a superposition of a non-vertical translation and a rotation around the centre of mass of the reflector. The former effect can be characterized by a horizontal velocity component v . The latter, by an angular velocity ω . Both $\dot{v} = 0$ and $\dot{\omega} = 0$, since,

apart from air friction, the motion after launch is unperturbed. These velocity components give rise to the two disturbing effects, which will be discussed in the remainder of this Section.

A. Centripetal acceleration

The free-fall acceleration is referred to the centre of mass CM of the flying body, whereas the tracked trajectory relates to the optical centre OC of the reflector, i.e., the apparent point at which the optical path is reversed. During the launching phase, the bending moment of the launch pad makes the reflector rotate around CM. We will (realistically) neglect twisting components, so that, during the flying phase, the rotation axis lies in a horizontal plane. Since in practice the optical centre does not coincide with the centre of mass, OC is subjected to a centripetal acceleration towards CM. The vertical component of this acceleration, a_{cent} , superposes to the free-fall acceleration g (fig. 1).

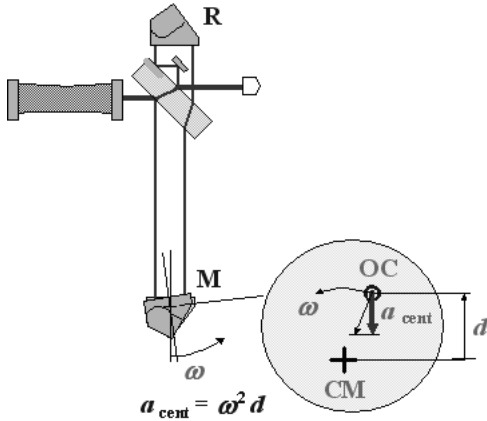


Fig. 1. The centripetal acceleration.

By denoting with d the vertical position of OC with respect to CM, one has

$$a_{cent} = \omega^2 d, \quad (1)$$

where ω is the angular velocity. Strictly speaking, a_{cent} varies along the circular path of OC. However, the path during the flight corresponds to a so short rotation angle that the variation is negligible. We estimate to be able to balance the reflector in such a way that $-0.05 \text{ mm} \leq d \leq +0.05 \text{ mm}$. Therefore, the degree of knowledge concerning d is represented by a uniform probability density function (pdf), on the interval -0.05 mm and $+0.05 \text{ mm}$.

The rotation of the moving reflector is evaluated by illuminating its entering face with a high-power laser beam and marking on a piece of white paper the final position of the spot traced during the flight by the weakly reflected beam, as shown in fig. 2.

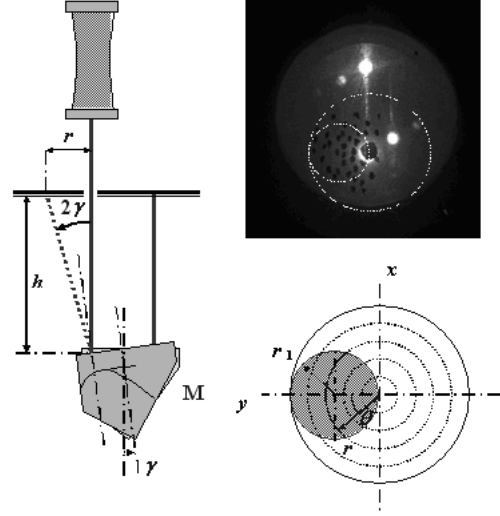


Fig. 2. Optical system used to detect the test body rotation.

The rotation angle γ is thus calculated as:

$$\gamma \approx \frac{r}{2h}, \quad (2)$$

where r is the distance of the spot from the optical axis and $h = 300 \text{ mm}$ is the distance between the white paper and the reflector at the end of its flight.

By repeating the launch, one can have a visual representation of the scatter of the spots, from which a pdf for r , and eventually for γ , can be inferred. For the IMG02 setup the typical scatter, as shown in fig. 2, is roughly represented by a bivariate uniform density over a circle of radius $r_1 = 8 \text{ mm}$.

The joint pdf for the Cartesian coordinates x and y of the spot is

$$f(x, y) = \begin{cases} \frac{1}{\pi r_1^2} & x^2 + y^2 - 2 r_1 y \leq 0 \\ 0 & \text{elsewhere} \end{cases}. \quad (3)$$

By passing to polar coordinates r and θ , and integrating over θ , the marginal pdf for r is

$$f(r) = \begin{cases} \frac{2}{\pi r_1^2} \arccos\left(\frac{r}{2r_1}\right) & 0 \leq r \leq 2 r_1 \\ 0 & \text{elsewhere} \end{cases}. \quad (4)$$

The angular velocity ω is related to r by

$$\omega = \frac{r}{2ht}, \quad (5)$$

where $t = 0.4$ s is the flying time. The pdf for ω is easily obtained from eqs. (4) and (5).

The pdf for the rotation angle γ is derived from eqs. (2) and (4) (fig. 3). The expectation of γ is about 0.015 rad, i.e., 0.9° .

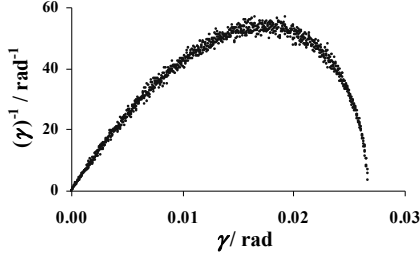


Fig. 3. Distribution of the rotation angle γ .

To this value would correspond in the worst case ($|d| = 0.05$ mm) a value of a_{cent} equal to $7 \mu\text{Gal}$.

B. Coriolis acceleration

The East-West component v_{EW} of the parasitic horizontal velocity v of the test body induces on it a vertical component a_{Cor} of the Coriolis acceleration, according to:

$$a_{\text{Cor}} = 2\omega_E v_{\text{EW}} \sin(\pi/2 - \varphi), \quad (6)$$

where $\omega_E = 7.29 \cdot 10^{-5} \text{ rad} \cdot \text{s}^{-1}$ is the Earth's angular velocity and φ is the (known) latitude of the measurement site [7]. This acceleration component superposes to the free-fall acceleration. To evaluate the magnitude of the Coriolis effect, it is necessary to evaluate v_{EW} . By establishing a suitable reference frame, we write $v_{\text{EW}} = v \sin \beta$, where β is the angle between the North and the direction of v (fig. 4).

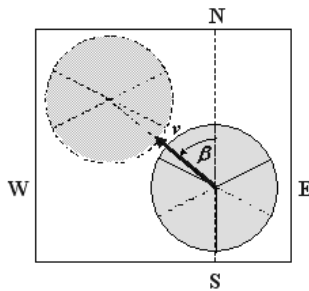


Fig. 4. Direction of the horizontal motion of the test body.

As concerns the angle β , at present the IMGC-02 does not adopt a system to detect this direction, therefore our knowledge on β is represented by a uniform distribution on the interval $-\pi$ and $+\pi$.

The term v can be evaluated experimentally. To this purpose, we remark that any horizontal displacement of the moving reflector determines a misalignment of the optical

system. This results in a decrease of the initial amplitude A_0 of the interference signal.

We intentionally misaligned one of the reflectors by displacing it horizontally by known distances δ_i , and recorded the resulting amplitudes A_{δ_i} of the interference signal.

Fig. 5 shows the curve obtained by fitting a second-order polynomial to the relative amplitudes A_{δ_i}/A_0 thus observed with the IMGC-02 setup.

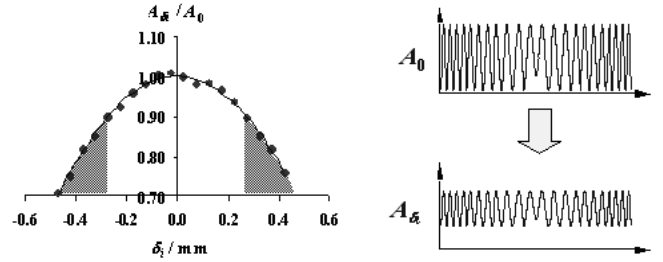


Fig. 5. Left: relative fringe amplitude vs horizontal displacement of the test body (shaded areas correspond to rejected launches). Right: interference signals from aligned (top) and misaligned (bottom) conditions.

The displacement δ of the test body at the end of the trajectory during routine measurements is calculated by inverting the fitting polynomial and turns out to be

$$\delta = \sqrt{\frac{(1 - A_{\delta}/A_0)}{1.343}}. \quad (7)$$

The corresponding velocity v is computed by dividing this displacement by the observation time (for experimental reasons, this time is typically equal to about 0.3 s, thus smaller than the total flying time [6]):

$$v = \frac{\delta}{t_{\text{obs}}}. \quad (8)$$

We made about 2000 launches and constructed the empirical frequency distribution of the variation of the relative amplitude $(1 - A_{\delta}/A_0) = \xi$ (fig. 6).

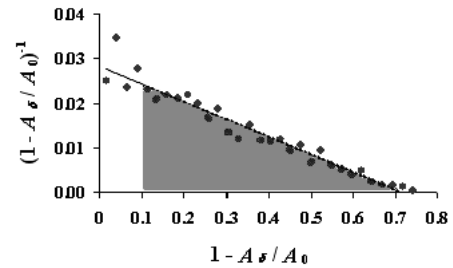


Fig. 6. Frequency distribution of the variation of the fringe amplitude (shaded area corresponds to rejected launches).

This empirical frequency distribution is representative of that obtained from real experimental data during routine measurement sessions. The corresponding pdf is obtained by smoothing the empirical frequency distribution with a straight line:

$$f(\xi) = \begin{cases} -3.98 \cdot 10^{-2} \xi + 2.85 \cdot 10^{-2} & 0 \leq \xi \leq 0.717 \\ 0 & \text{elsewhere} \end{cases} \quad (9)$$

The upper limit of the pdf is due to the limited ability of the acquisition system to process noisy interference signals.

The corresponding distribution of the displacement δ is derived from eqs. (7) and (9) using the Monte Carlo method, and is given in fig 7.

The expectation is about 0.4 mm. To this value would correspond in the worst case ($|\beta| = \pi/2$ and $\varphi = 0$) a value of a_{Cor} equal to 19 μGal . Although this is a worst-case value, estimates would be anyway affected by a significant, unknown bias (being β unknown) that could not be reduced by repeating the measurements.

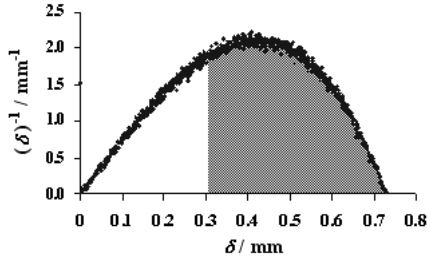


Fig. 7. Distribution of the displacement δ of the test body (shaded area corresponds to rejected launches).

To keep this bias within acceptable limits, in routine measurements, those launches for which $\delta > 0.3$ mm are rejected. This amounts to reject most of the launches, as shown in fig. 6. The distribution of δ is therefore truncated (the rejected part is represented by the shaded area in fig. 7). The remaining distribution has an expectation equal to about 0.2 mm, corresponding in the worst-case to a bias of about 9 μGal .

IV. MEASUREMENT UNCERTAINTY

The measurand in gravimetry is the free-fall acceleration g . The quantity measured in the i th launch with IMGC-02 is the difference a_i between the accelerations of the optical centres of the moving and reference reflectors during the flight of the former.

$$a_i = a_{iM} - a_{iR} \quad (10)$$

In an ideal setup, the acceleration a_{iR} should be equal to zero. In practice, the filtering of parasitic vibrations from the ground floor is imperfect and some disturbances reach the

reference reflector, despite the care taken to isolate it. Although the spectrum of these disturbances is far from being simple, and still subject to investigation, for the purposes of this study it is sufficient to consider them as normally distributed, with zero mean and standard deviation equal to some tens of microgal, the value depending on the specific measurement site. For the IMGC-02 instrument working at the INRIM gravity laboratory, the typical value, well confirmed by experimental evidence, is about 30 μGal .

As concerns a_{iM} , it is the sum of the free-fall acceleration g and of the two parasitic accelerations we are studying, that is, a_{cent} and a_{Cor} . g is traditionally intended as the resultant of the Newtonian and centrifugal components only. In addition, in a_{iM} are embedded a number of other contributions, arising from tides and many other effects. These contributions are not relevant here, since they can be taken into account with negligible uncertainty. Therefore we write

$$a_{iM} = g + a_{\text{cent}} + a_{\text{Cor}} \quad (11)$$

By combining eqs. (10) and (11), and writing explicitly the various contributions from eqs. (1) and (6), one has

$$a_i = g + \omega_i^2 d + 2\omega_E v_i \sin \beta \sin(\pi/2 - \varphi) - a_{iR} \quad (12)$$

Incidentally, this equation, concerning an individual launch, shows which quantities vary and which remain constant among repeated launches.

As already mentioned, the free-fall acceleration measured value is taken as the average of N launches, (typically $N=200$), one tenth of the overall number of trials, as explained in Sec. III-B. The purpose of this Section is the evaluation of the uncertainty associated with the measured value, in order to form the *measurement result* [8, 2.9], therefore we will consider the equation

$$\varepsilon = \bar{a} - g = \overline{\omega^2 d} + 2\omega_E \bar{v} \sin \beta \sin(\pi/2 - \varphi) - \bar{a}_R \quad (13)$$

which expresses the estimate error as a function of the contributing components. This expression is site-dependent through the second and third terms in the right-hand side of eq. (13). Our analysis will refer to the site of the INRIM gravity laboratory.

To study the pdf of this error, following [3], the pdfs of the input quantities are propagated through model (13) to form the pdf of the output quantity. The recommended “propagation tool” is the Monte Carlo method (MCM). This method is well suited to the present application, whereas the GUM uncertainty framework would lead to dubious results or, in the least, would be difficult to apply. Actually, the first-order approximation of model (13) would miss some of the contributions to the uncertainty, as both the expectations of d and $\sin\beta$ are zero. The necessary second-order terms would be cumbersome to evaluate for Gaussian pdfs [9]. Finally, no expression is known for them if the pdfs of the concerned quantities are not Gaussian, as in this case.

The expectation and standard deviation of ω^2 are obtained from eqs. (4) and (5) by a first Monte Carlo simulation. They are equal to $1.67 \cdot 10^{-3} \text{ rad}^2 \cdot \text{s}^{-2}$ and to $1.16 \cdot 10^{-3} \text{ rad}^2 \cdot \text{s}^{-2}$, respectively. The corresponding values for v are obtained in the same way from eqs. (7), (8) and (9), and are equal to $5.98 \cdot 10^{-4} \text{ m} \cdot \text{s}^{-1}$ and $2.16 \cdot 10^{-4} \text{ m} \cdot \text{s}^{-1}$, respectively. As concerns a_R , as already mentioned, its pdf is Gaussian with zero mean and standard deviation equal to $30 \text{ } \mu\text{Gal}$. Thanks to the Central Limit Theorem, the pdfs of $\overline{\omega^2}$, \overline{v} and $\overline{a_R}$ are approximately Gaussian, with the same expectation and variance reduced by the square root of N (typically $N = 200$).

The pdf assigned to d in Sec. III-A is a uniform with zero mean and standard deviation equal to $0.05/\sqrt{3}$. The pdf for $\sin\beta$ is an arcsine (U-shaped) distribution with expectation zero and variance $1/\sqrt{2}$ [3]. By further using MCM, the pdfs of the individual contributions and of the overall error are numerically simulated (fig. 8).

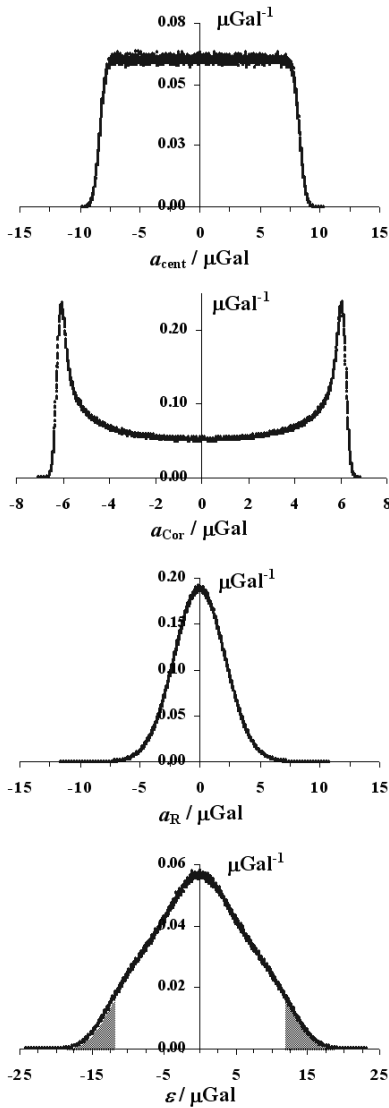


Fig. 8. Pdfs of the individual contributions and of the overall measurement error.

Beside the inverse transform method, recommended in Supplement 1 (and implemented in Labview), also the acceptance-rejection method (see, e.g., [10]) (implemented in R) was applied for validation purposes, obtaining the same results. All the pdfs have expectation vanishingly low. Therefore, as anticipated, the centripetal and Coriolis accelerations, as modelled in this study, do not affect the measured value and only contribute to its uncertainty. The standard deviations are $4.8 \text{ } \mu\text{Gal}$ and $4.4 \text{ } \mu\text{Gal}$, respectively.

That of a_R is, as expected, $2.1 \text{ } \mu\text{Gal}$. The resulting standard deviation of typical measured free-fall acceleration is $6.8 \text{ } \mu\text{Gal}$. The pdf is highly symmetric, so that the shortest and the probabilistically symmetric coverage intervals virtually coincide. The endpoints of the 95% coverage interval are $-12.9 \text{ } \mu\text{Gal}$ and $+12.9 \text{ } \mu\text{Gal}$.

V. CONCLUSIONS

We analyzed two disturbing effects in absolute ballistic gravimetry. These effects are not detected in routine measurements, and their evaluation requires dedicated tests as well as the application of advanced techniques in uncertainty evaluation. We showed that the contribution of these effects to the uncertainty associated with free-fall acceleration is dominating. On-line detection of these effects and their correction is a challenge for future improvements in ballistic gravimetry and, as such, deserves further investigations.

REFERENCES

- [1] T. M. Niebauer, G. S. Sasagawa, J. E. Faller, R. Hilt and F. Klopping, "A new generation of absolute gravimeters". *Metrologia*, Vol. 32, pp. 159-180, 1995.
- [2] G. D'Agostino, "Development and metrological characterization of a new transportable absolute gravimeter". *PhD thesis*, Polytechnic of Turin, Italy, 2005.
- [3] BIPM, IEC, IFCC, ILAC, ISO, IUPAC, IUPAP and OIML. Evaluation of measurement data, Supplement 1 to the "Guide to the expression of uncertainty in measurement" - Propagation of distributions using a Monte Carlo method, JCGM 101, International Organization for Standardization, Geneva, 2008.
- [4] A. Germak, S. Desogus and C. Origlia, "Interferometer for the IMGC rise-and-fall absolute gravimeter". *Metrologia*, Vol. 39, pp. 471-475, 2002.
- [5] G. D'Agostino, A. Germak, S. Desogus and G. Barbato, "A method to estimate the time-position coordinates of a free-falling test-mass in absolute gravimetry". *Metrologia*, Vol. 42, pp. 222-228, 2005.
- [6] W. Bich, G. D'Agostino, A. Germak and F. Pennecci, "Uncertainty Propagation in a Non-linear Regression Analysis: Application to a Ballistic Absolute Gravimeter (IMGC-02)". *Proc. Workshop AMUEM07 ed. IEEE I&M* (cd rom), 2007.
- [7] M. Alonso and E.J. Finn, "Physics". *Addison-Wesley*, 1992.
- [8] BIPM, IEC, IFCC, ILAC, ISO, IUPAC, IUPAP and OIML. International Vocabulary of Metrology---Basic and General Concepts and Associated Terms, VIM, 3rd Edition. International Organization for Standardization, Geneva, 2007.
- [9] G. Mana, F. Pennecci, "Uncertainty propagation in non-linear measurement equations", *Metrologia*, Vol. 44, pp. 246-251, 2007.
- [10] G. S. Fishman, "Monte Carlo: concepts, algorithms and applications", *Springer Series in Operations Research*, 1996.